forests

MDPI

Article

First Results of a Geometric Morphometric Analysis of the Leaf Size and Shape Variation in *Quercus petraea* Across a Wide European Area

Paola Fortini [1,2], Elisa Proietti [3,*], Srdjan Stojnic [4], Piera Di Marzio [1,2], Filippos A. Aravanopoulos [5], Raquel Benavides [6,7], Anna Loy [1] and Romeo Di Pietro [2,3]

[1] Department of Bioscience and Territory, University of Molise, 86090 Pesche, Italy; fortini@unimol.it (P.F.); piera.dimarzio@unimol.it (P.D.M.); a.loy@unimol.it (A.L.)
[2] NBFC, National Biodiversity Future Center, 90133 Palermo, Italy; romeo.dipietro@uniroma1.it
[3] Department of Planning, Design, and Technology of Architecture University of Rome Sapienza, 00196 Rome, Italy
[4] Institute of Lowland Forestry and Environment, University of Novi Sad, Antona Čehova 13, 21000 Novi Sad, Serbia; stojnics@uns.ac.rs
[5] Faculty of Agriculture, Forestry and Natural Environment, Aristotle University of Thessaloniki, 51124 Thessaloniki, Greece; aravanop@for.auth.gr
[6] Department of Natural Systems and Resources, Escuela Técnica Superior de Ingeniería de Montes, Forestal y del Medio Natural, Universidad Politécnica de Madrid (UPM), C/José Antonio Novais 10, 28040 Madrid, Spain; raquel.benavides@upm.es
[7] Centro para la Conservación de la Biodiversidad y el Desarrollo Sostenible (CBDS-UPM), C/José Antonio Nováis, 10, 28040 Madrid, Spain
* Correspondence: elisa.proietti@uniroma1.it

Abstract: The high leaf morphological variability of European white oaks is largely documented in the botanical literature, and several papers have been published in the last two decades focusing on inter- and intraspecific leaf phenotypic plasticity. Studies involving landmark-based geometric morphometrics proved to be useful in highlighting relationships between leaf size and shape variation and environmental factors, phylogenetic patterns, or hybridization events. In this paper, the leaf size and shape variations of 18 populations of *Quercus petraea* distributed throughout a wide geographical area were analyzed by means of geometric morphometric methods (GMMs). This study involved 10 European countries and investigated the intraspecific leaf variability of *Q. petraea* within a wide latitudinal and longitudinal gradient. Analyses of variance for shape and centroid size were performed through Procrustes ANOVA. Multivariate analysis procedures, partial least squares method, and regression analyses were used to highlight possible patterns of covariation between leaf shape and size and geographical/environmental variables. The results revealed that the *Q. petraea* populations analyzed mainly differed in their leaf size, where a decrease was observed according to a north to south geographical gradient. Both leaf size and shape were found to be significantly related to latitude, and, to a lesser extent, to mean annual temperature and the leaf isotopic signature of ^{15}N. All the other variables considered did not provide significant results. Unexpected differences observed comparing the leaf traits of geographically strictly adjacent populations suggest the involvement of local hybridization/introgression events. However, with a few exceptions, *Q. petraea* turned out to be quite conservative in its leaf shape and size at both the local and continental scale.

Keywords: biogeography; geometric morphometric (GMM); leaf traits; latitudinal gradient; white oaks

check for updates

Academic Editor: Fei-Hai Yu

Received: 15 October 2024
Revised: 6 December 2024
Accepted: 27 December 2024
Published: 4 January 2025

Citation: Fortini, P.; Proietti, E.; Stojnic, S.; Di Marzio, P.; Aravanopoulos, F.A.; Benavides, R.; Loy, A.; Di Pietro, R. First Results of a Geometric Morphometric Analysis of the Leaf Size and Shape Variation in *Quercus petraea* Across a Wide European Area. *Forests* **2025**, *16*, 70. https://doi.org/10.3390/f16010070

1. Introduction

There is plenty of evidence that multiple genes simultaneously regulate leaf morphology [1,2] and that environmental and climatic factors may also play an important role [2–6]. Analyzing variation in leaf shape and size may allow us to understand in which way some of the processes take place, leading plants to adapt to the surrounding environmental conditions and, in particular, to climate [7–11]. Furthermore, it is well known that variations in leaf size and shape have a strong impact on the rates at which plants photosynthesize [12–15]. This knowledge can guide the design of efficient management procedures or conservation plans for safeguarding species and communities. Leaf morphology has been widely studied, especially in taxonomy and ecology, based on traditional macro- and micro-morphometric analyses. However, in the last two decades, geometric morphometric techniques (GMMs) have gained more and more attention [16–22]. GMMs, unlike traditional approaches, enable separate analyses of the size and shape variation of a set of objects based on a set of morphological landmarks (corresponding to Cartesian coordinates of points that can be precisely located on the specimens under study (e.g., [23–27])). Specifically, the process known as Procrustes superimposition enables the alignment and comparison of the shapes of different objects by removing non-shape variations such as size, position, and orientation [8,26,28–30]. Multivariate analyses of shape can then be carried out using the shape coordinates of the superimposed landmarks to explore various biological questions [1,26], such as comparative studies among populations. Numerous studies of spatial variation in leaf size and shape are available in the botanical literature, especially at the regional or even more local scales [31–33]. In fact, recent evidence highlighted the relevant role of the intraspecific variability underlying ecological processes [34–37]. In general, plant species with a wide geographical distribution generally show wide intraspecific variation [38–41]. In this study, we explored variation in the leaf form of *Quercus petraea* (Matt.) Liebl., a well-known white oak species that bears considerable ecological, coenological, and economic importance in Europe [42]. This species exhibits a wide distribution in western Eurasia and plays a dominant or co-dominant role in many European oak forest ecosystems [43]. *Q. petraea*, commonly known as sessile oak, is widely distributed from southern Norway and Sweden to the northern part of the Iberian Peninsula, South Italy, the Balkan Peninsula, and Anatolia [44]. Accordingly, *Q. petraea* can be considered a good choice for investigating the underlying mechanisms of intraspecific leaf size and shape variation at a large scale. Due to its high phenotypic plasticity and broad genetic variability, amplified by frequent hybridization and introgression with other white oak species, *Q. petraea* can adapt and thrive in a variety of climatic and edaphic conditions [45,46]. As is already known, leaf morphology provides the basic information for oak species identification, and this also applies to the *Q. petraea* collective group whose real (or presumed) taxonomic variability (and critical issues) is mainly based on some morphological traits of the leaves, such as the sinus depth, gibbosity of the acorn cupule, and hairiness degree of the abaxial leaf blade [47–51]. The morphometric studies on the leaf variability in *Q. petraea* that have already been published address this issue at a regional or, at most, a national scale [18,51]. In many cases, these were aimed at comparing the leaf traits of *Q. petraea* to those of other sympatric white oak species [51]. However, delving into the leaf variability in *Q. petraea* across a wide latitudinal and longitudinal transect involving the majority of *Q. petraea*'s range allows for the acquisition of information and provision of new data on the relationships between *Q. petraea* leaf morphology, and several environmental factors, the majority of which are linked to the geographical distribution of the populations investigated. Since it is known that leaf form directly responds to mechanisms for acclimation and adaptation, intraspecific spatial variation helps to predict species distribution, persistence, and dispersal. It is, therefore, hoped that this type of study may be of some use in the near future to shed light on possible adaptation mechanisms used by this species to face global climate change. In particular, the use of GMMs combined with the measurement of some morphological traits of leaves enables a focus on the variations in shape, freeing analyses from some dimensional parameters that could vary significantly depending on the seasonal climate trend. The aim of this study is, therefore, to investigate the variability in *Q. petraea* populations in terms of morphometric leaf traits in response to environmental gradients. In particular, we analyzed the variation in leaf shape and size across 18 populations distributed throughout 10 European countries covering a wide latitudinal and longitudinal range.

2. Materials and Methods

2.1. Plant Materials

This research analyzed 3784 leaves from 419 trees across 18 populations of *Quercus petraea* (Matt.) Liebl. The goal was to examine the variations in leaf size and shape within the species using geometric morphometric methods (GMMs). This research covered a large European area, including 10 countries: France, Germany, Italy, Lithuania, Norway, Poland, Spain, Sweden, Switzerland, and the United Kingdom. The *Q. petraea* leaves' collection was carried out as a part of the GenTree project (EU-Horizon 2020, [52]), aimed at characterizing the genetic and phenotypic variability in forest tree species to optimize the management and sustainable use of forest genetic resources [53]. Within the GenTree project, populations were sampled in local pairs (except for Lithuania and Poland) where two populations per single locality were selected across a local gradient (such as elevation and water availability) but with significant potential for gene flow. However, in this study, not all the populations were considered in pairs, since some specimens of one of the two populations were found to be too damaged to be used for the GMMs measurements (Table 1, Figure 1). An average of 9 leaves per tree were collected from a fully lit branch from the top of the crown selecting those without visible herbivory or other damage and subsequently scanned to assess leaf area. They were then oven-dried at 60 °C for 72 h, ground, and analyzed for carbon and nitrogen content (C:N, no units) and isotope ^{13}C and ^{15}N content in plant material (δ ^{13}C, δ ^{15}N reported relative to V-PDB, ‰). Leaf collection, storage, processing, and morphological trait measurement followed Pérez-Harguindeguy et al. [54], while the chemical analyses were carried out using gas chromatography–combustion isotope ratio mass spectrometry (GC-C-IRMS) at the UC Davis Stable Isotope Facility (https://stableisotopefacility.ucdavis.edu/ accessed on 13 April 2020). All this information is available in Benavides et al. [53].

Table 1. Populations of *Quercus petraea* investigated by means of GMM analysis.

Population ID	Country	Site of Collection	Latitude (°N)	Longitude (°E)	Altitude (m)
ES01	Spain	Moncayo	41.79575	−1.78664	1066
ES02	Spain	Moncayo	41.79682	−1.78208	964
FR03	France	Vouillè	46.60473	0.17268	154
FR04	France	Moulière	46.65091	0.47727	137
CH05	Switzerland	Berg am Irchel-Hochwacht	47.55579	8.57907	652
CH06	Switzerland	Berg am Irchel-Irchelebni	47.55622	8.59093	666
IT07	Italy	Tatti	43.34902	10.97555	432
IT08	Italy	Monterufoli	43.24305	10.78558	500
IT10	Italy	Aspromonte	38.14434	15.93818	1592

Table 1. *Cont.*

Population ID	Country	Site of Collection	Latitude (°N)	Longitude (°E)	Altitude (m)
GB11	United Kingdom	Roudsea	54.23332	−3.02858	21
NO13	Norway	Skiftenes	58.41064	8.48852	102
NO14	Norway	Nedre Timenes	58.16645	8.12551	83
SE15	Sweden	Fogdaröd	55.9265	13.5943	101
SE16	Sweden	Kolleberga-Ekbacken	56.06721	13.27396	57
DE17	Germany	Siehdichum	52.17070	14.47502	75
DE18	Germany	Fünfeichen	52.17021	14.47549	114
PL19	Poland	Nidzica	53.39086	20.40111	199
LT20	Lithuania	Veisejai-Seirijai	54.23331	23.75621	177

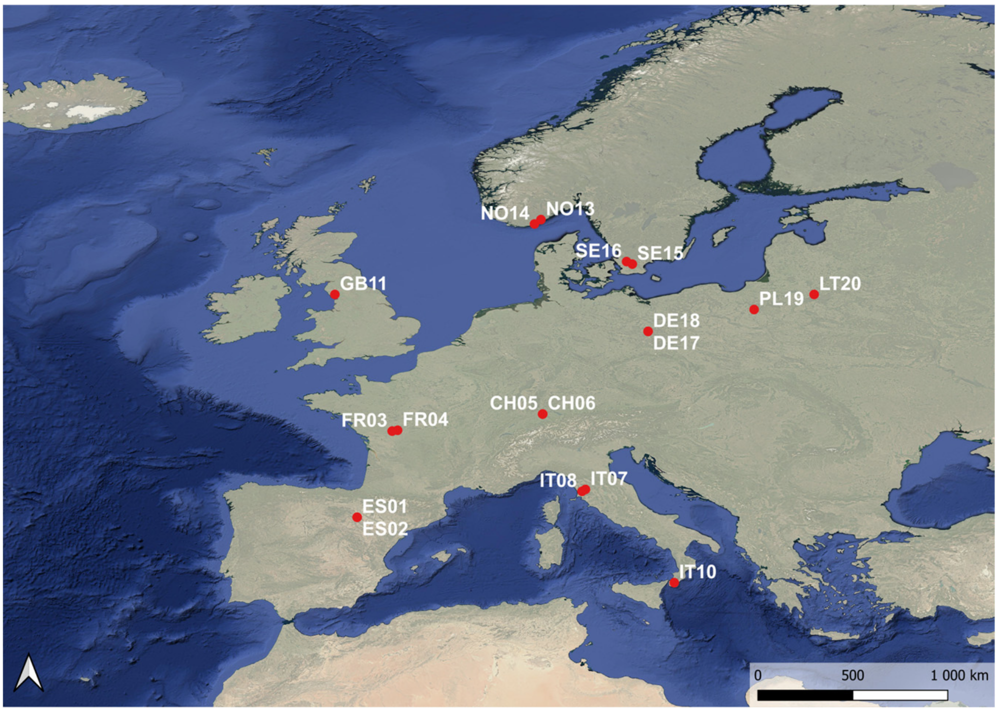

Figure 1. Distribution map of sample localities (Map data ©2015 Google).

2.2. Landmarks Configuration

We captured the main features of the leaf shape by measuring 13 two-dimensional landmarks (LMs) on both sides of the leaf, according to a procedure carried out in previous studies on oaks [20,21,55,56]. Both unpaired and paired landmarks were considered [57].

The first ones (LMs 1–3) were located along the middle axis of the leaf, while the second ones (LMs 4–13) were placed on both sides of the leaf (Figure 2).

The Tps Series software [58,59] was used for digitizing and capturing the x, y Cartesian coordinates of images of each leaf. Three sets of coordinates (matrices) were created and processed: (a) the "leaf matrix", which includes the coordinates of all the 3784 leaves; (b) the "tree matrix", which contains averaged coordinates of leaves per landmark and per tree (419 trees); and (c) the "population matrix", which consists of the averaged coordinates of leaves per landmark and per population (18 populations).

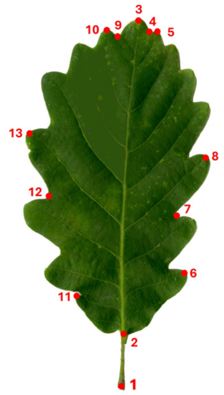

1	Base of the petiole
2	Petiole – leaf blade junction
3	Apex of the leaf blade
4, 9	Base of the sinus immediately below the apex of the leaf blade
5, 10	Tip of the lobe immediately below the apex of the leaf blade
8, 13	Tip of the lobe at the largest width of the leaf blade
7, 12	Base of the sinus immediately below the lobes of the landmarks 8 and 13, respectively
6, 11	Tip of the first basal lobe, starting from the petiole

Figure 2. Configuration of the 13 leaf blade landmarks (in red in the image) used in GMM analysis.

2.3. Morphometric Analyses of Leaf Variation

The leaf morphology was analyzed using Morpho J version 1.08.01 [26] and R packages (ape, ggplot2, stats, and tidyverse), in R version 4.3.3 [60–62]. At first, we performed a Generalized Procrustes Analysis (GPA) to separate the original coordinates of the leaf morphology into two new matrices, i.e., shape variables and centroid size values. The centroid size represents a measure of size and is calculated as the square root of the sum of the squared distances of all landmarks from their centroid of the object [8,28,63]. We used the Procrustes fitting to convert the raw landmark coordinate matrix of the 3784 leaves considered into a normalized shape matrix. GPA resulted in an optimal superimposition of landmark configurations (Figure 3).

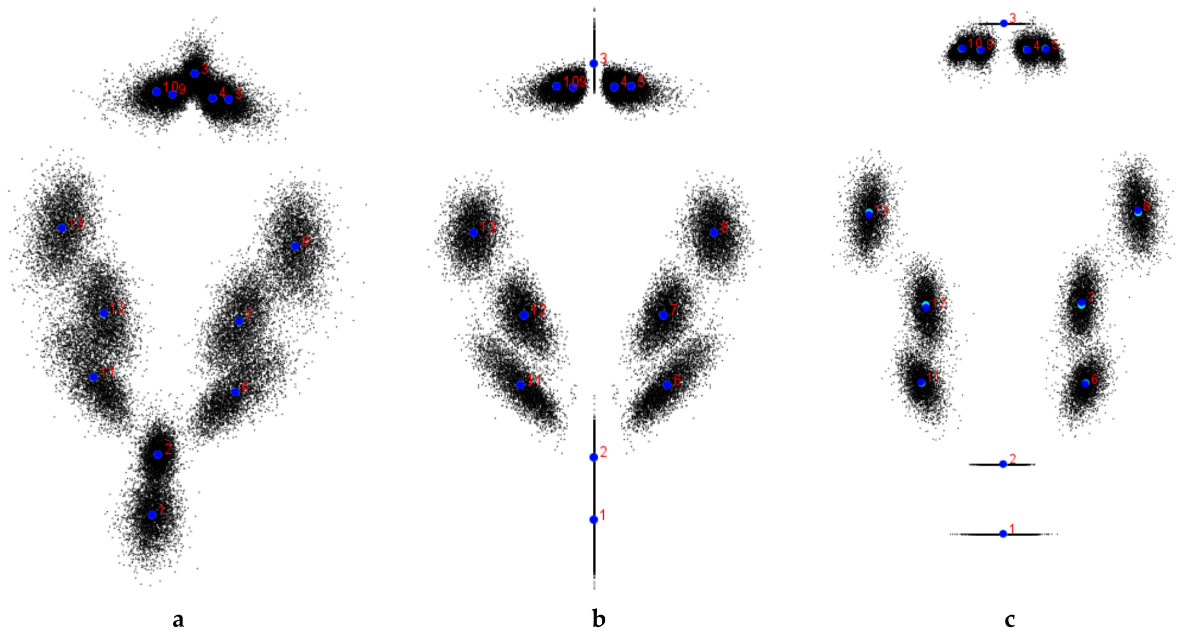

Figure 3. Generalized Procrustes Analysis (GPA) of the leaf shape of *Quercus petraea* based on the coordinates of the 13 landmarks using: (**a**) full raw coordinate matrix, (**b**) GPA symmetric component of shape, and (**c**) GPA asymmetric component of shape. The blue dots represent the mean landmark positions, and the small black dots represent the landmark positions for individual configurations in the sample.

Outliers were detected through MorphoJ, based on the Mahalanobis distances among leaves, which calculates how much the shape of each sampled leaf differs from the average shape [64,65]. The outlier's identification process highlighted 14 leaves that deviated from the average leaf profile. These leaves were, therefore, removed from further analyses

(Table S1). A wireframe graph representing a stylized leaf that was created by connecting lines among landmarks. To evaluate the amount of leaf shape and size variation among trees and populations, a Procrustes ANOVA on shape variables and an ANOVA on centroid size were performed, respectively. The centroid size variation in the population was represented via box plots, and their differences were tested via an ANOVA and subsequent post hoc test (Tukey–Kramer).

A principal component analysis (PCA) was performed on the shape variables to display which leaf traits (derived from the LMs' position) were involved in driving shape variations across individuals, trees, and populations. A dendrogram of phenotypic relationships was carried out using UPGMA (unweighted pair group method with arithmetic mean) on the Mahalanobis distances. The latter distances were also used to quantify shape distances among leaves, trees, and populations. Differences in leaf size were analyzed only among trees and populations.

2.4. Relationship Between Sets of Variables and Leaf Morphology

We analyzed the correlation between the symmetric components of the mean leaf shape of each population (block 1) and the geographical and environmental variables of the sampling sites (block 2) using the two-Block Partial Least Squares (2B-PLS) analysis. We also used a regression analysis to assess the covariation between geographical and environmental variables and leaf size. The following parameters were considered: geographical: latitude (°N), longitude (°E), and altitude (m); ecological: soil depth (cm), stone content (categorical variable), rock cover (categorical variable), solar radiation (kJ/m^2), temperature (°C), precipitation (mm/year), mean relative humidity of the growing season (April–October) (no unit), aridity (no unit), and isothermality (no unit). In addition, the specific leaf area (SLA, mm^2/mg) was investigated and the following chemical variables of the leaves were considered: C:N (no unit), $\delta\ ^{13}C$ (‰), and $\delta\ ^{15}N$ (‰) (Table S2). All these data are published in Opgenoorth et al. [52] and Benavides et al. [53].

3. Results

3.1. Analyses of the Leaf Shape

A Procrustes ANOVA applied on the leaf shape showed significant effects of population and directional asymmetry (DA, i.e., the tendency in bilateral structures of one side to always prevail on the other as the result of specific adaptive pressures) on leaf shape variation ($F = 42.87$; $p < 0.0001$, and $F = 25.07$; $p < 0.0001$), whereas fluctuating asymmetry (FA, i.e., the portion of the shape variation in bilateral structures that affects, independently, the left and right sides) was not significant (Table 2). Also, the effect of population was much higher than the effect of DA (Table 2), suggesting a relatively marginal influence of the latter. Thus, further analyses were only focused on leaf shape variation among populations.

Principal component analysis (PCA) performed on the symmetric components of the leaf shape, considering both the "leaf matrix" and "tree matrix", showed a significant overlap of the leaf shape among the populations considered. Accordingly, no discontinuities among populations along the main PCs were observable in the two scatterplots (see Figures S1 and S2). The scatterplot of the first three PC scores computed on the symmetric components of the leaves showed a light pattern of variation (87.41% of cumulative variance) among populations (Figure 4). Indeed, a light leaf shape variation is identifiable by looking at the wireframe graphs showing the difference between the average shape (the light blue outline), which represents the mean shape in the sample of 18 populations, and the target shape (the dark blue outline) that represents the shape change of interest (here, it is associated with the position of each population in the first three principal components). The most significant shape variations were recorded along PC1, which captures the variation in petiole length and the leaf blade width. A general shortening of the petiole, a shrinkage of the basal part of the leaf, and a widening of the upper part of the leaf emerged when moving from the negative to the positive end of the axis.

Table 2. Results from Procrustes ANOVA on leaf shape analyzed at the population level. DA = directional asymmetry; FA = fluctuating asymmetry; SS: Procrustes sum of squares; MS: Procrustes mean squares; df: degrees of freedom; F: Goodall's F statistics; *p* (param.): parametric *p*-values.

	Shape (Dimensionless Procrustes Units)				
	SS	**MS**	**df**	**F**	***p* (Param.)**
Population	6.7409	0.0360	187	42.87	<0.0001
DA	0.2319	0.0211	11	25.07	<0.0001
FA	0.1572	0.0008	187	0.9	0.8432
Residual	77.4828	0.0009	82,544		

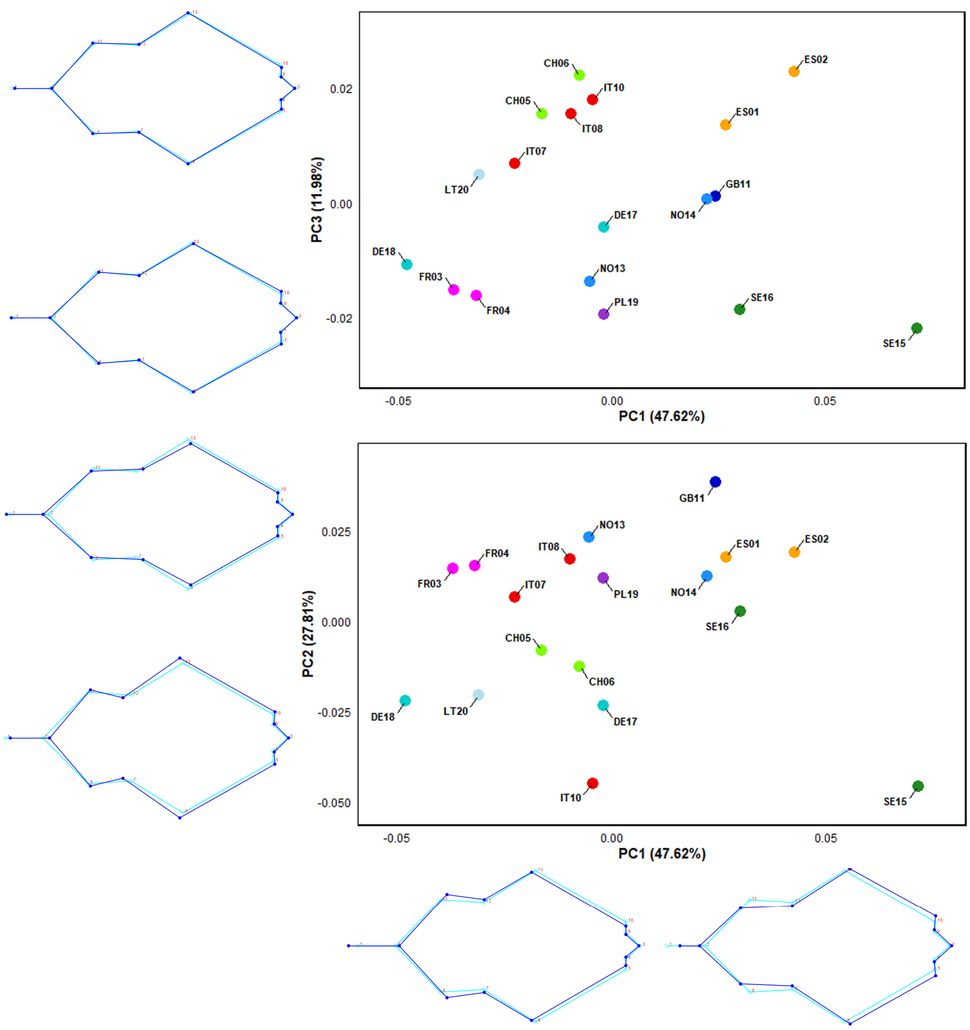

Figure 4. PCA scatter plots showing the mean leaf shape variation in the 18 populations of *Quercus petraea*. The scatter plots show the first three PCs (PC1, PC2, and PC3), which, overall, explain 87.41% of the variance. The wireframe graphs represent the extreme mean leaf shapes along the PCs. The target shape, colored in dark blue, is displayed for the scale factor of −0.05 and + 0.07 along PC1, −0.05 and + 0.04 along PC2, and −0.02 and +0.02 along PC3, while the general mean shape is colored in light blue. Populations from the same country are colored with the same color (CH: chartreuse; DE: cyan; ES: orange; FR: magenta; IT: red; LT: lightblue; NO: dodgerblue; PL: darkorchid; SE: forestgreen; GB: blue).

The Mahalanobis distances were calculated to quantify the differences in leaf shape among populations. The results showed that the greatest Mahalanobis distance value (4.39) was found between the Swedish population SE15 and the French one FR04, the lowest (0.63) was found between the two Spanish populations (ES01 and ES02) (Figure 5). The relationships among population leaf shapes are shown in the phenogram generated from UPGMA cluster analysis based on the Mahalanobis distances (Figure 6).

	CH05	CH06	DE17	DE18	ES01	ES02	FR03	FR04	GB11	IT07	IT08	IT10	LT20	NO13	NO14	PL19	SE15	SE16
CH05		<0.0001	<0.0001	<0.0001	<0.0001	<0.0001	<0.0001	<0.0001	<0.0001	<0.0001	<0.0001	<0.0001	<0.0001	<0.0001	<0.0001	<0.0001	<0.0001	<0.0001
CH06	0.88		<0.0001	<0.0001	<0.0001	<0.0001	<0.0001	<0.0001	<0.0001	<0.0001	<0.0001	<0.0001	<0.0001	<0.0001	<0.0001	<0.0001	<0.0001	<0.0001
DE17	1.85	1.65		<0.0001	<0.0001	<0.0001	<0.0001	<0.0001	<0.0001	<0.0001	<0.0001	<0.0001	<0.0001	<0.0001	<0.0001	<0.0001	<0.0001	<0.0001
DE18	1.24	1.50	1.73		<0.0001	<0.0001	<0.0001	<0.0001	<0.0001	<0.0001	<0.0001	<0.0001	<0.0001	<0.0001	<0.0001	<0.0001	<0.0001	<0.0001
ES01	2.47	2.16	2.34	**3.06**		0.0011	<0.0001	<0.0001	<0.0001	<0.0001	<0.0001	<0.0001	<0.0001	<0.0001	<0.0001	<0.0001	<0.0001	<0.0001
ES02	2.39	2.10	2.32	**3.11**	0.63		<0.0001	<0.0001	<0.0001	<0.0001	<0.0001	<0.0001	<0.0001	<0.0001	<0.0001	<0.0001	<0.0001	<0.0001
FR03	1.28	1.30	1.80	0.98	**2.56**	**2.63**		<0.0001	<0.0001	<0.0001	<0.0001	<0.0001	<0.0001	<0.0001	<0.0001	<0.0001	<0.0001	<0.0001
FR04	1.52	1.60	2.12	1.19	**3.02**	**3.03**	0.77		<0.0001	<0.0001	<0.0001	<0.0001	<0.0001	<0.0001	<0.0001	<0.0001	<0.0001	<0.0001
GB11	1.86	1.99	1.63	2.31	1.77	1.64	1.96	2.32		<0.0001	<0.0001	<0.0001	<0.0001	<0.0001	<0.0001	<0.0001	<0.0001	<0.0001
IT07	1.20	1.52	1.92	0.89	**2.87**	**2.86**	1.08	1.11	2.07		<0.0001	<0.0001	<0.0001	<0.0001	<0.0001	<0.0001	<0.0001	<0.0001
IT08	1.23	0.99	1.66	1.31	2.51	2.46	0.95	1.13	1.99	1.03		<0.0001	<0.0001	<0.0001	<0.0001	<0.0001	<0.0001	<0.0001
IT10	**3.04**	**2.63**	2.23	**2.70**	**3.70**	**3.72**	**2.86**	**2.78**	**3.48**	**2.73**	2.29		<0.0001	<0.0001	<0.0001	<0.0001	<0.0001	<0.0001
LT20	1.66	1.51	1.25	1.46	**2.86**	**2.86**	1.62	1.94	2.22	1.85	1.53	2.34		<0.0001	<0.0001	<0.0001	<0.0001	<0.0001
NO13	1.57	1.75	1.51	1.58	2.31	2.29	1.39	1.70	1.46	1.28	1.33	**2.73**	1.85		<0.0001	<0.0001	<0.0001	<0.0001
NO14	1.51	1.65	1.32	1.86	1.97	1.82	1.78	2.07	1.04	1.59	1.63	**2.94**	1.98	0.93		<0.0001	<0.0001	<0.0001
PL19	1.44	1.40	1.21	1.37	2.39	2.31	1.23	1.56	1.58	1.47	1.33	**2.75**	1.48	1.09	1.07		<0.0001	<0.0001
SE15	**3.89**	**3.69**	**2.78**	**4.15**	**3.07**	**2.90**	**4.11**	**4.39**	**3.02**	**4.19**	**3.95**	**4.09**	**3.88**	**3.40**	**2.82**	**3.21**		<0.0001
SE16	2.30	2.10	1.11	2.39	2.06	1.92	2.21	2.51	1.38	2.39	2.15	**2.92**	2.12	1.64	1.17	1.29	2.13	

Figure 5. Mahalanobis distances [64] among the populations of *Quercus petraea* derived from shape variables (below the diagonal) and *p*-values from multivariate permutation tests (10,000 permutation rounds) using Pillai's trace (above the diagonal). The color code shows the Mahalanobis distance from low (green) to high (red) values.

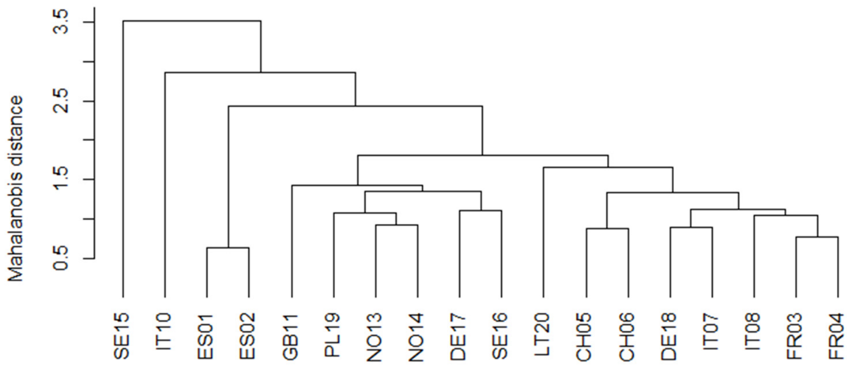

Figure 6. UPGMA tree derived from the Mahalanobis distances of shape variables for the 18 populations of *Quercus petraea* analyzed.

3.2. Centroid Size Variation

An ANOVA applied on the centroid size displayed an effect of population on the size variation (F = 109.97; $p < 0.0001$). In addition, a higher percentage of variance was expressed by "within population" differences compared to "among populations" (Table 3).

The variation in centroid size among populations (Figure 7) allowed us to distinguish two major groups of populations having CS values lower (GR1: from 109.59 to 136.06 mm) and higher (GR2: from 147.66 to 176.5 mm) than the average value (142.51 mm), respectively (see Table S3). The highest increment among mean values of the CS (13.6) was recorded between populations FR03 and FR04, while the second one (11.6) was between IT07 and GB11. All other increments between adjacent populations on the graph were found to be much smaller and not statistically significant (Table S3). On the basis of the average value of the centroid size, the increment between IT07 and GB11 was here considered as the separation threshold between two major groups which can be distinguished by latitude. These groups can broadly be considered as a Mediterranean–oceanic one distributed in western and southern Europe and a boreal–temperate one distributed in central-eastern and northern Europe. Results for leaf shape and size variation for each population are summarized in Figure 8.

Table 3. Results from ANOVA on centroid size: SS: sums of squares; MS: mean squares; df: degrees of freedom; F: F statistics; *p* (param.): parametric *p*-values.

	Centroid Size (mm)					
	SS	**MS**	**df**	**F**	***p* (Param.)**	**Variance Component (%)**
Among population	1,432,749.5859	84,279.3874	17	109.97	<0.0001	34.26%
Within population	2,875,347.6621	766.3507	3752			65.74%

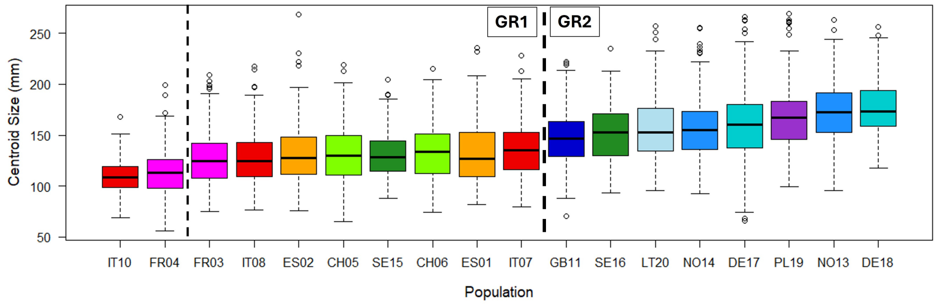

Figure 7. Boxplots showing the variation in centroid size values (mm) for the 419 trees belonging to the 18 populations analyzed. Boxes represent the interquartile range (IQR, 25th to 75th percentiles), the bold black line inside each box is the median, and the whiskers cover $\pm$ 1.5 $\times$ IQR. Circles indicate outliers. Populations are sorted by increasing the mean value of the centroid size. The dotted line separates populations belonging to the group 1 (GR1) and group 2 (GR2). The same color code of Figure 4 is used.

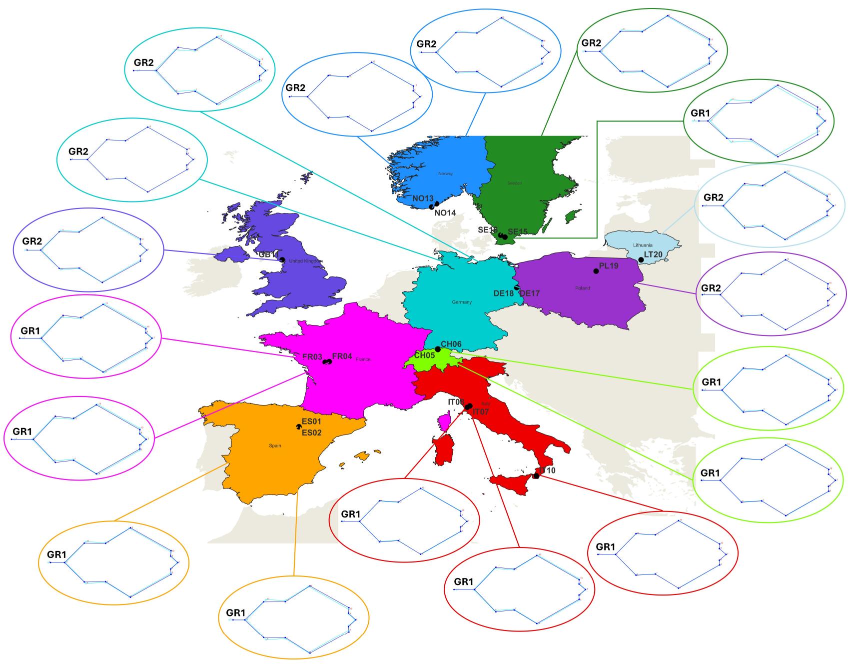

Figure 8. Leaf shape and size variations of the 18 populations of *Quercus petraea*. The wireframe graphs of the symmetric components represent the leaf shapes along PC1 (landmark are in the same order of Figure 2). The same color code of Figure 4 is used. GR1 and GR2 are the two main groups of populations identified through the result of the ANOVA on the centroid size.

3.3. Relationships Between Sets of Variables and Leaf Shape

The results of the 2B-PLS analysis showed that there was a significant relationship between the symmetric components of the leaf shape and geographic gradient expressed by the latitude and altitude of populations (RV: 0.1578; r: 0.76; *p*-value: 0.0043) (Figure 9), as well as with the δ [15]N leaf content (RV: 0.6233; r: 0.87; *p*-value: <0.0001) (Figure 10). Differently, the relationship between the symmetric components of the leaf shape and all the other parameters analyzed was found to be not significant (see Figure S3). Leaf shape variation showed a subtle change along a lower-to-higher altitude gradient which was found to be roughly corresponding to that observable along a higher-to-lower latitude gradient. In detail, moving along this gradient, from a negative to positive value in block 1 PLS1, a general shortening of the petiole and widening of the basal and middle part of the leaf was observed. Leaf shape variation was more evident considering the δ [15]N content. The wireframe graphs showed a general shortening of the petiole and shrinkage of the basal part of the leaf connected to a widening of the upper part of the leaf in the condition of high values of the δ [15]N (left part of the block 1 PLS1).

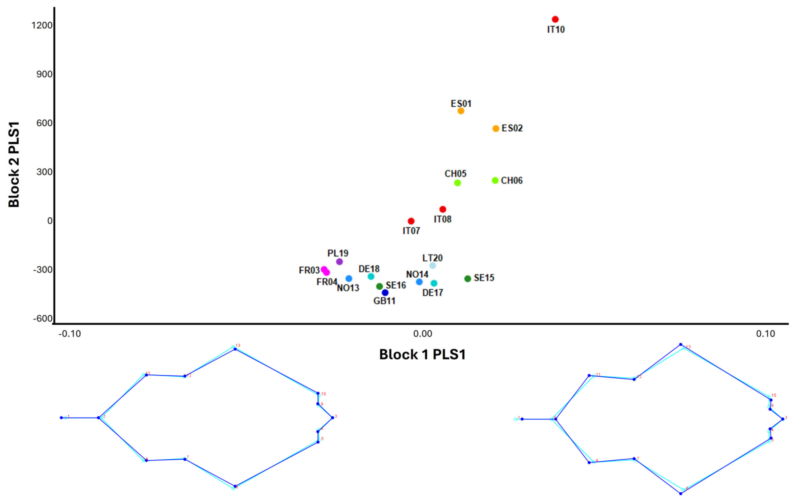

Figure 9. Scatterplots of the 2B-PLS analysis showing the relations between altitude and latitude (Block 2 PLS1) and the symmetric components of the shape (Block 1 PLS1) of the leaves of *Quercus petraea* studied. The wireframe graphs represent the leaf shapes at the negative (−0.025) and positive (+0.04) extremes of the PLS1 axis. RV: 0.1578; r: 0.76; *p*-value: 0.0043. The same color code of Figure 4 is used.

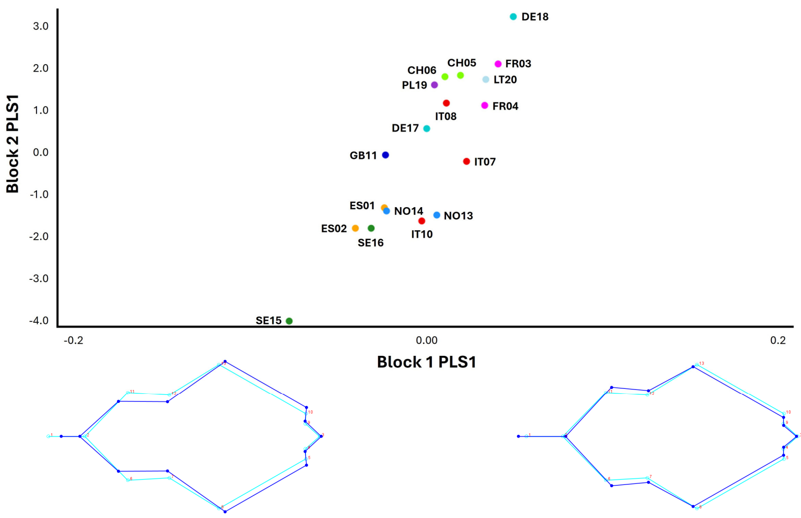

Figure 10. Scatterplots of the 2B-PLS analysis showing the relations between the δ [15]N content in the leaves (block 2 PLS1) and the symmetric components of the shape (block 1 PLS1) of the leaves of *Quercus petraea* studied. The wireframe graphs represent the leaf shapes at the negative (−0.08) and positive (+0.05) extremes of the PLS1 axis. The same color code as Figure 4 is used. RV: 0.6233; r: 0.87; *p*-value: <0.0001.

3.4. Relationships Between Sets of Variables and Leaf Size

We found a significant relation between leaf centroid size and latitude (R squared = 0.569, *p*-value = 0.0003), as well as between leaf size and mean annual temperature (R squared = 0.517, *p*-value = 0.0008). In contrast, the relationship between leaf size and all the other parameters was not significant (see Figure S4). A progressive increase in the centroid size value was found moving from the lower-to-higher latitudes and from higher-to-lower mean annual temperatures (Figure 11a,b).

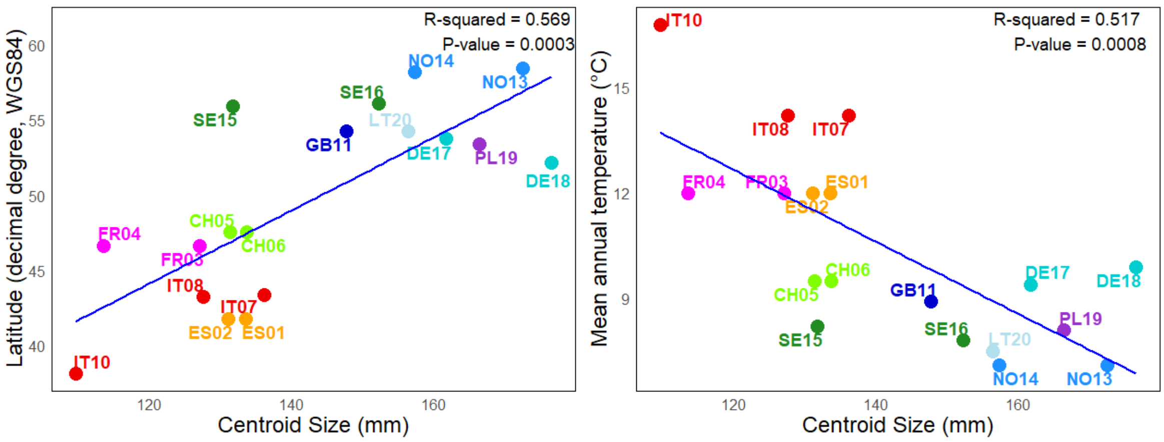

a **b**

Figure 11. (**a**): regression of the centroid size values (mm) of each *Quercus petraea* population analyzed on the latitude (decimal degree, WGS84); (**b**): regression of the centroid size values (mm) of each *Quercus petraea* population analyzed on the mean annual temperature (°C) (1985–2015). The same color code of Figure 4 is used.

4. Discussion

Clinal variation over a latitudinal gradient has been documented in several fields, such as phenology, growth, sexual reproduction, responses to herbivory, and even genes' neutral DNA sequences [40,66–72], among widespread plant species. In this study, we explored the intraspecific variation in leaf shape and size of *Quercus petraea* to identify patterns of differentiation across wide geographical and environmental gradients in Europe. Previous studies showed that *Q. petraea* natural populations exhibit significant levels of genetic and phenotypic variability [73,74]. We assumed that the contrasting differences in the climatic/environmental features of the sites of collection located so far (e.g., Scandinavia vs. southern Italy or Spain vs. Lithuania) would have had a significant impact on the development and growth of the trees and, therefore, would also be reflected in the morphological characteristics of the leaf. Our results, based on geometric morphometric analyses, only partially confirmed this assumption. In fact, despite the large range of latitudes and longitudes of the sample sites, we found slight differences in leaf shape and only a little more marked differences in the leaf size of the populations considered. These results are in contrast, for example, to the leaf shape variation documented for the *Quercus pubescens* complex, whose notoriously significant variability is the triggering factor responsible for the description of a still undefined number of taxa, or presumed ones (see [75–81]).

It is possible that the sampling design conducted within the GenTree project based on paired *Q. petraea* populations with contrasting environmental conditions at the local scale blurred our expectation about finding more significant differences in leaf shape at a larger scale. In fact, even contrasting conditions within single pairs of local populations did not seem to have resulted in significant differences (at least in terms of variations in the leaf shape). This was probably due to the fact that some topographic/environmental parameters (e.g., altitude, parent material, and slope) of the two sampling sites for the same locality did not significantly differ from each other. Among the few exceptions, in this regard, there are the two Swedish populations of *Q. petraea*. These populations showed significant differences in terms of leaf shape despite being collected in sites displaying largely similar topographical and environmental conditions, except, maybe, for the altitude (see Table 1 and Table S2 and [53]). One of the two populations (SE16) is located at 57 m a.s.l., while the other (SE15) is located at 101 m. As reported in Rydin et al. [82], the distribution of the vegetation in Sweden is more dependent on elevation than on latitude where moderate differences in altitude outside the mountains are able to significantly influence the floristic and coenological pattern. Accordingly, it is possible that a difference of fifty meters in altitude, whose impact on environmental conditions would be considered negligible in southern Europe, could instead be significant at much higher latitudes like those of south Sweden (which incidentally coincides with the overall northernmost limit of the distribution of *Q. petraea*). However, the detected differences in the leaf shape between the two Swedish sessile oak populations do not necessarily have to be associated with differences in the environmental or topographical features of the sites. Other reasons could also be involved, such as those concerning events of hybridization and backcrossing, which have been found to be quite common among white oaks [83–86]. If we take these introgressive hybridization events as plausible also for the Swedish *Q. petraea* populations in issue, the only possibility (as partner species) would be to involve *Quercus robur* L., the only other white oak species occurring in southern Scandinavia and by far the most abundant. On the other hand, hybridization and backcrossing between *Q. petraea* and *Q. robur* are well documented in the tree genetic literature of central and northern Europe [85,87–89]. Comparing the leaf shape of these two Swedish populations, it was observed that the individuals of SE15 show a significantly shorter petiole and narrower and an elongated leaf base. Both these leaf traits could be considered as plausible with a genetic "contamination" by *Q. robur* (or, at least, to a higher degree of genetic contamination with *Q. robur* with respect to that affecting the other Swedish *Q. petraea* population). Unfortunately, we lack usable genetic data to confirm or refute this theory.

A deeper insight into the results showed a positive correlation between the leaf shape and two geographical parameters (altitude and latitude). In more detail, we found that the leaf shape displayed, on average, a greater width of the base of the leaf and a shorter petiole for increasing latitudes and (less evidently) for decreasing altitudes (Figure 9). This result should be taken with care, since we have no evidence showing which factors, physical or ecological, underlie the aforementioned leaf-shape gradient. Similarly, we do not have sufficient information to explain another statistically significant correlation that emerged in this study, namely the correlation between the leaf shape and the leaf isotopic signature of ^{15}N (Figure 10). In this case, the higher isotopic signature of ^{15}N in the leaf corresponded to a leaf-shape gradient towards shorter petioles, narrower base, and wider middle part of the leaves. In fact, the abundance of plant ^{15}N isotopic signatures is studied mainly at the level of ecosystem functionality as it provides valuable information on the spatial–temporal patterns of these nitrogen cycling and loss processes in ecosystems [90] where bulk soil and foliar $\delta^{15}N$ were found to be positively related [91]. While leaf $\delta^{15}N$ was found to be a reliable indicator of the ecophysiological behavior of plants [92,93], there are currently no studies that relate this factor to possible variations in leaf morphology. Only by cross-referencing these data with other data deriving from further types of analyses (environmental, eco-physiological, genetic, etc.) will it be possible to verify whether this morphometric evidence could be suitable to be explained through scientific reasoning based on factual data.

Perhaps more consistent are the gradients identified in the correlations between some geographical parameters and the leaf size. Namely, a significant correlation was highlighted for latitude, where the *Q. petraea* populations from southern Europe were found to be smaller on average than those from northern Europe. A confirmation of this result was provided by another significant correlation that we found, which involves the mean annual temperature, a variable known to be directly and closely related to latitude. In contrast, no significant correlation was found between leaf size and mean annual rainfall.

Observing the diagram of variation for the leaf centroid size (Figure 7), it is evident that an increasing dimensional trend passing from the population of Aspromonte (the southernmost tip of the Italian Peninsula) to those of north Germany and south Norway is observable. A division into two (three) main groups of sessile oak populations is observable and statistically confirmed by an ANOVA (Table S3). The first division, which runs between the two French populations of *Q. petraea*, cannot be easily explained. This separation could be related to the strictly topographical context, rather than to the regional ones. At present, we can only classify it as an "anomalous" centroid size "jump" within a more-or-less continuous trend of increase in this parameter observable along the latitudinal gradient. Probably, a denser sampling in this French area and/or in the strictly surrounding ones would have helped to fill the centroid size dimensional gap highlighted in the diagram. Otherwise, as already aforementioned for the two Swedish populations, we could again refer to possible hybridization events that would have asymmetrically affected the two French populations or exclusively affected one population and not the other. Even in this case, as in the previous one, only through the support of targeted genetic analyses will it be possible to have a more precise response to what has just been hypothesized. In this case, however, not only would *Q. robur* be the potential hybridizing species but *Q. pubescens* too, so that identifying possible intermediate morphological traits considering the three potential taxa involved would be a more complex issue (see Fortini et al. [51]).

The second division, observable in the diagram of variation for the leaf centroid size, separates the population set approximately into two groups, of which one is composed exclusively of populations of southern Europe (GR1), and one is composed of the populations from central–northern Europe (GR2). This separation was statistically confirmed by an ANOVA and is observable on the geographic map in Figure 8, where a clear geographical separation of the populations into two groups is evident based on the centroid-size value being higher or lower than the average value. The only exception is the Swedish population already mentioned above (SE15), which, with a centroid size lower than the average, is positioned in the southern European group of populations (GR1). The peculiarity of SE15 also emerges in the UPGMA cluster analysis of the matrix based on a canonical analysis of Procrustes coordinates of the leaf shape, where this population represents the one most isolated from all the others.

The southern European group exhibits a higher degree of climatic heterogeneity than the central–northern group since two climatic macro-regions (namely the Mediterranean and the temperate one) and nine climatic variants are involved in GR1, whereas one macroclimatic region (namely the temperate one) and three climatic variants are involved in GR2 (see Rivas-Martínez et al. [94]). In fact, it would be enough to look at the table reporting the raw data of temperature and precipitation of the sites belonging to the two groups (Table S2) to quantify the aforementioned bioclimatic differences. Accordingly, the two French populations coming from central–western France and the Swiss populations from the northern side of the Alps have very little to do with the Italian or Spanish populations in terms of climate features. However, a reading on a very broad geographical scale, such as the one used in this study, allows us to accept, at least in part, such an "unlikely" grouping. In broad terms, we could say that the two groups outlined in the boxplot include the following: the Mediterranean–oceanic populations (southern European group) and the temperate–boreal populations (central–north European group). If we try to read this division according to a taxonomic key, we could say that the "northern group" of sessile oak populations occupies an area that is shared exclusively with *Quercus robur* populations while the "southern group" of sessile oak populations occupies an area completely enclosed within the distribution limits of *Q. pubescens* and various other taxa belonging to the collective group of the downy oaks [81,95]. Moreover, for the southern Italy population, the occurrence of *Q. frainetto* Ten. must also be considered [96,97], while for the Spanish populations, two other additional white oaks are present, namely *Q. faginea* Lam. and *Q. pyrenaica* Willd. [98]. We cannot actually know whether the influence of the genome of the Mediterranean pubescent downy oaks together with those of *Q. frainetto*, *Q. faginea*, and *Q. pyrenaica* to the south and that of *Q. robur* to the north may have played a discriminating role in the establishment of the identified leaf morphology gradient. At present, we can only report what we observed and raise some points of interest which could hopefully be explored in the future.

According to some authors, the positive correlation between leaf size and the latitude/temperature binomial can be related to eco-physiological reasons [99,100]. In fact, under conditions of high solar radiation and low water availability or low stomatal conductance, smaller leaves help to maintain adequate leaf temperatures and higher photosynthetic water-use efficiency by reducing boundary layer resistance [101]. Additionally, in sunny habitats, smaller leaves are expected to have lower leaf temperatures than larger leaves in order to prevent overheating [102].

As regards oaks, and in particular the *Q. petraea* populations, the relationship between leaf morphology and climatic or geographical parameters have already been investigated in the past both at a large and small scale. Among the small-scale studies, Bruschi et al. [46] highlighted that the leaves of the Sicilian populations exhibited smaller leaves than those of the populations from central Italy, justifying this result with the greater light radiation characterizing the Sicilian *Q. petraea* populations. Other small-scale studies found positive correlations between leaf size vs. aridity with smaller leaves occurring in dryer sites [103]. The result found by Fortini et al. [104] analyzing *Q. pubescens* populations distributed along a transect traced from the Tyrrhenian coast to the Apennine ridge moves apparently in a slightly opposite direction with smaller leaves found to be associated with the montane (and presumably moister, but also colder) sites. In that case, it is very likely that the cold winter winds and thin soils where *Q. pubescens* is relegated when it occurs at its upper altitudinal limit may play a key role in discriminating a small-leaved morphotype.

5. Conclusions

This study aimed to analyze, through geometric morphometrics techniques, the variation in the leaf size and shape of 18 European *Quercus petraea* populations and showed that this variation was especially present at the level of leaf size and only to a lesser extent at the level of leaf shape. The most significant evidence was that related to the variation in the centroid size which exhibited increasing values according to the increasing latitude. The occurrence of hybrids between *Quercus petraea* and *Q. robur* in one of the two Swedish populations was hypothesized owing to the presence of intermediate morphological diagnostic traits between these two taxa. In general, the *Q. petraea* leaf turned out to be a remarkably conservative element, reflecting only a minor influence from geographic and environmental parameters. It showed a very low variation in shape associated to a slightly higher variation in size, throughout a large geographic area ranging in latitude from southern Italy to southern Sweden. It is possible that more significant variations in the leaf size and shape of *Q. petraea* could be discovered by including in the sampling design a higher number of populations especially from Eastern Europe (e.g., Czech Republic, Slovakia, and Hungary) and the Balkans. In these two European sectors, *Q. petraea* acts a notoriously highly variable species either from the morphological or ecological point of view, so that a high number of critical taxa are currently comprised in its collective group, i.e., *Q. banatus* Kucera, *Q. dalechampii* Auct., and *Q. polycarpa* Schur, which are often placed in synonymy with *Q. petraea* s.s. but on which full light has not yet been shed [50,104–109]. The inclusion of populations from the Balkan area would represent an essential requirement in the study of the leaf variability in *Q. petraea*. Indeed, the Balkan, Italian, and Iberian Peninsulas have represented the main refugee sites for European white oaks during the glaciations and are some of the sites of conservation of white oaks and, in general, of the whole deciduous forest biome, during the glaciations [110–115], and are some of the most diversified areas from a genetic and phylogeographical point of view [113–119]. For the same reason, in order to outline an overall scheme of the leaf variability in *Q. petraea*, the Caucasus cannot be left out. In addition to *Q. petraea* s.s., this area is characterized by the occurrence of some closely related taxa (e.g., *Q. petraea* subsp. *dshorochensis* (K.Koch) Menitsky and *Q. petraea* subsp. *iberica* (Steven ex M.Bieb.) Krassiln.) and by other potentially hybridizing white oaks, such as *Q. robur*, *Q. hartwissiana* Steven, and *Q. macranthera* Fisch. et C.A. Mey. ex Hohen [120,121]. Highly important, finally, would be to analyze oak material from areas of high biogeographical importance such as Anatolia and Iran (the latter being the current eastern-most limit of distribution of *Q. petraea*), for which some data have already been published on the GMM features of local white oak populations [122,123].

Supplementary Materials: The following supporting information can be downloaded at https://www.mdpi.com/article/10.3390/f16010070/s1: Table S1: List of the 14 outliers identified and removed from the GMM analyses; Table S2: Geographical and environmental variables considered in the study. Lat—latitude (°N, WGS84), Lon—longitude (°E, WGS84), Alt—altitude (m), SD—soil depth (cm), SC—stone content (categorical variable), RC—rock cover (categorical variable), SR—solar radiation (kJ/m^2), T—mean annual temperature (°C), P—annual sum of precipitation (mm), RH—relative humidity of the growing season (April—October) (no unit), A—aridity (no unit), I—isothermality (no unit), C:N—ratio between carbon and nitrogen (unitless), δ^{13}C—isotopic signature of stable ^{13}C isotope (‰), δ^{15}N—isotopic signature of stable ^{15}N isotope (‰) (sources: Benavides et al. 2021; Opgenoorth et al. 2021); Figure S1: PCA scatter plot of the 18 populations of *Quercus petraea* based on the symmetric components of the leaf shape of the "leaf matrix"; Figure S2: PCA scatter plot of the 18 populations of *Quercus petraea* based on the symmetric components of the leaf shape of the "tree matrix"; Table S3: ANOVA on the Centroid size (CS) values of the 18 populations analysed; Figure S3: Scatterplots of the 2B-PLS analysis showing the relations between the geographical and environmental parameters considered (Block 2 PLS1) and the symmetric components of the shape (Block 1 PLS1) of leaves of *Quercus petraea* studied; Figure S4: Regression of the centroid size values of each *Quercus petraea* population analyzed on the geographical and environmental parameters studied.

Author Contributions: Conceptualization, P.F., S.S. and R.D.P.; validation, E.P., P.F., P.D.M., S.S. and R.D.P.; investigation, P.F., E.P., P.D.M., S.S., F.A.A., R.B., A.L. and R.D.P.; data curation, E.P., P.F., S.S. and P.D.M.; writing—original draft preparation, P.F., E.P., P.D.M. and R.D.P.; writing—review and editing, P.F., E.P., S.S., P.D.M., F.A.A., R.B., A.L. and R.D.P.; visualization: E.P. and P.D.M.; supervision, P.F. and R.D.P.; project administration, P.F. and R.D.P. All authors have read and agreed to the published version of the manuscript.

Funding: This study was partially supported by: (a) MUR PRIN 2022, project code: 2022B3HA72 (PI. R. Di Pietro, UO P. Fortini) CUP B53D23011890006. (b) the National Recovery and Resilience Plan (NRRP), Mission 4 Component 2: Investment 1.4, Call for tender No. 3138 of 16 December 2021, rectified by Decree n.3175 of 18 December 2021 of the Italian Ministry of University and Research; Award Number: project code CN_00000033, Concession Decree No. 1034 of 17 June 2022 adopted by the Italian Ministry of University and Research, Project funded by the European Union "NextGenerationEU NBFC"; R. Di Pietro: CUP B83C22002950007; P. Fortini and P. Di Marzio CUP H73C22000300001; project title "National Biodiversity Future Center". This study was also partially supported by: (c) the General Secretariat of Research and Innovation, Greece, through the Aristotle University of Thessaloniki (Project No. 74167, PI: F.A. Aravanopoulos). (d) the Spanish Ministry of Science and Innovation with project 'FORTRESS' (PID2021-127241OB-I00, PI: R. Benavides). (e) the Ministry of Science, Technological Development and Innovation of the Republic of Serbia (Contract No. 451-03-66/2024-03/200197) and the European Union's Horizon 2020 research and innovation program under grant agreement No. 676876 (GenTree).

Data Availability Statement: The data presented in this study are available on request from the corresponding author.

Conflicts of Interest: The authors declare no conflicts of interest.

References

1. Klingenberg, C.P. Evolution and development of shape: Integrating quantitative approaches. *Nat. Rev. Genet.* **2010**, *11*, 623–635. [CrossRef] [PubMed]
2. Fu, G.; Dai, X.; Symanzik, J.; Bushman, S. Quantitative gene–gene and gene–environment mapping for leaf shape variation using tree-based models. *New Phytol.* **2017**, *213*, 455–469. [CrossRef] [PubMed]
3. Barkoulas, M.; Galinha, C.; Grigg, S.P.; Tsiantis, M. From genes to shape: Regulatory interactions in leaf development. *Cur. Opin. Plant Biol.* **2007**, *10*, 660–666. [CrossRef]
4. Fritz, M.A.; Rosa, S.; Sicard, A. Mechanisms underlying the environmentally induced plasticity of leaf morphology. *Front. Genet.* **2018**, *9*, 478. [CrossRef]
5. Guerin, G.R.; Wen, H.; Lowe, A.J. Leaf morphology shift linked to climate change. *Biol. Lett.* **2012**, *8*, 882–886. [CrossRef]
6. Li, Y.; Zhang, Y.; Liao, P.C.; Wang, T.; Wang, X.; Ueno, S.; Du, F.K. Genetic, geographic, and climatic factors jointly shape leaf morphology of an alpine oak, *Quercus aquifolioides* Rehder & E.H. Wilson. *Ann. For. Sci.* **2021**, *78*, 64. [CrossRef]
7. Dryden, I.L.; Mardia, K.V. *Statistical Analysis of Shape*; John Wiley & Sons: Chichester, UK, 1998.
8. Mitteroecker, P.; Gunz, P.; Windhager, S.; Schaefer, K. A brief review of shape, form, and allometry in geometric morphometrics, with applications to human facial morphology. *Hystrix It. J. Mamm.* **2013**, *24*, 59–66. [CrossRef]
9. Li, Y.; Zou, D.; Shrestha, N.; Xu, X.; Wang, Q.; Jia, W.; Wang, Z. Spatiotemporal variation in leaf size and shape in response to climate. *J. Plant Ecol.* **2020**, *13*, 87–96. [CrossRef]
10. Stojnić, S.; Viscosi, V.; Marković, M.; Ivanković, M.; Orlović, S.; Tognetti, R.; Cocozza, C.; Vasić, V.; Loy, A. Spatial patterns of leaf shape variation in European beech (*Fagus sylvatica* L.) provenances. *Trees* **2022**, *36*, 497–511. [CrossRef]
11. Wang, H.; Wang, R.X.; Harrison, S.P.; Prentice, I.C. Leaf morphological traits as adaptations to multiple climate gradients. *J. Ecol.* **2022**, *110*, 1344–1355. [CrossRef]
12. Brito-Rocha, E.; Schilling, A.C.; Dos Anjos, L.; Piotto, D.; Dalmolin, A.C.; Mielke, M.S. Regression models for estimating leaf area of seedlings and adult individuals of Neotropical rainforest tree species. *Braz. J. Biol.* **2016**, *76*, 983–989. [CrossRef] [PubMed]
13. Fonseca, C.R.; Overton, J.M.; Collins, B.; Westoby, M. Shifts in trait-combinations along rainfall and phosphorus gradients. *J. Ecol.* **2000**, *88*, 964–977. [CrossRef]
14. Malhado, A.C.M.; Whittaker, R.J.; Malhi, Y.; Ladle, R.J.; ter Steege, H.; Ramirez, H.A. Spatial distribution and functional significance of leaf lamina shape in Amazonian forest trees. *Biogeosciences* **2009**, *6*, 1577–1590. [CrossRef]
15. Shi, P.; Zhao, L.; David, A.; Ratkowsky, D.A.; Niklas, K.J.; Huang, W.; Lin, S.; Ding, Y.; Hui, C.; Li, B.L. Influence of the physical dimension of leaf size measures on the goodness of fit for Taylor's power law using 101 bamboo taxa. *Glob. Ecol. Conserv.* **2019**, *19*, e00657. [CrossRef]
16. Viscosi, V.; Fortini, P.; Slice, D.E.; Loy, A.; Blasi, C. Geometric morphometric analyses of leaf variation in four oak species of the subgenus Quercus (Fagaceae). *Plant Biosyst.* **2009**, *143*, 575–587. [CrossRef]
17. Viscosi, V.; Fortini, P. Leaf shape variation and differentiation in three sympatric white oak species revealed by elliptic Fourier analysis. *Nord. J. Bot.* **2011**, *29*, 632–640. [CrossRef]
18. Viscosi, V.; Antonecchia, G.; Lepais, O.; Fortini, P.; Gerber, S.; Loy, A. Leaf shape and size differentiation in white oaks: Assessment of allometric relationships among three sympatric species and their hybrids. *Int. J. Plant Sci.* **2012**, *173*, 875–884. [CrossRef]
19. Miljković, D.; Stefanović, M.; Orlović, S.; Stanković Neđić, M.; Kesić, L.; Stojnić, S. Wild cherry (Prunus avium (L.) L.) leaf shape and size variations in natural populations at different elevations. *Alp. Bot.* **2019**, *129*, 163–174. [CrossRef]
20. Proietti, E.; Filesi, L.; Di Marzio, P.; Di Pietro, R.; Masin, R.; Conte, A.L.; Fortini, P. Morphology, geometric morphometrics, and taxonomy in relict deciduous oaks woods in northern Italy. *Rend. Lincei* **2021**, *32*, 549–564. [CrossRef]

21. Yang, K.; Wu, J.; Li, X.; Pang, X.; Yuan, Y.; Qi, G.; Yang, M. Intraspecific leaf morphological variation in Quercus dentata Thunb.: A comparison of traditional and geometric morphometric methods, a pilot study. *J. For. Res.* **2022**, *33*, 1751–1764. [CrossRef]
22. De Luna-Bonilla, O.Á.; Valencia-Á, S.; Ibarra-Manríquez, G.; González-Rodríguez, A. Leaf morphometric analysis and potential distribution modelling contribute to taxonomic differentiation in the Quercus microphylla complex. *J. Plant Res* **2024**, *137*, 3–19. [CrossRef] [PubMed]
23. Ray, T.S. Landmark eigenshape analysis: Homologous contours; leaf shape in Syngonium (Araceae). *Am. J. Bot.* **1992**, *79*, 69–76. [CrossRef]
24. Bookstein, F.L. *Morphometric Tools for Landmark Data: Geometry and Biology*; Cambridge Univ. Press: Cambridge, MA, USA, 1991.
25. Klingenberg, C.P. Morphometrics and the role of the phenotype in studies of the evolution of developmental mechanisms. *Gene* **2002**, *287*, 3–10. [CrossRef]
26. Klingenberg, C.P. MorphoJ: An integrated software package for geometric morphometrics. *Mol. Ecol. Resour.* **2011**, *11*, 353–357. [CrossRef]
27. Shipunov, A.B.; Bateman, R.M. Geometric morphometrics as a tool for understanding Dactylorhiza (Orchidaceae) diversity in European Russia. *Biol. J. Linn. Soc.* **2005**, *85*, 1–12. [CrossRef]
28. Goodall, C.R. Procrustes methods in the statistical analysis of shape. *J. R. Stat. Ser. B (Stat. Methodol.)* **1991**, *53*, 285–339. [CrossRef]
29. Bookstein, F.L. Combining the tools of geometric morphometrics. In *Advances in Morphometrics*; Marcus, L.F., Corti, M., Loy, A., Naylor, G.J.P., Slice, D.E., Eds.; Plenum Press: New York, NY, USA, 1996; pp. 131–151.
30. Zelditch, M.L.; Lundrigan, B.L.; Garland, T., Jr. Developmental regulation of skull morphology. I. Ontogenetic dynamics of variance. *Evol. Dev.* **2004**, *6*, 194–206. [CrossRef]
31. Royer, D.L.; McElwain, J.C.; Adams, J.M.; Wilf, P. Sensitivity of leaf size and shape to climate within *Acer rubrum* and *Quercus kelloggii*. *New Phytol.* **2008**, *179*, 808–817. [CrossRef]
32. Jovanović, M.; Krekez Janković, I.; Milovanović, J.; Nonić, M.; Šijačić-Nikolić, M. Intraspecific variability of the sessile oak (*Quercus petraea* Matt. Liebl.) leaf traits from the Mount Kosmaj (Serbia). *Biol. Bull. Russ. Acad. Sci.* **2023**, *50*, 1223–1233. [CrossRef]
33. Jiang, F.; Cadotte, M.W.; Jin, G. Individual-level leaf trait variation and correlation across biological and spatial scales. *Ecol. Evol.* **2021**, *11*, 5344–5354. [CrossRef] [PubMed] [PubMed Central]
34. McGill, B.J.; Enquist, B.J.; Weiher, E.; Westoby, M. Rebuilding community ecology from functional traits. *Trends Ecol. Evol.* **2006**, *21*, 178–185. [CrossRef] [PubMed]
35. Albert, C.H.; Grassein, F.; Schurr, F.M.; Schurr, F.M.; Vieilledent, G.; Violle, C. When and how should intraspecific variability be considered in trait-based plant ecology? *Perspect. Plant Ecol. Evol. Syst.* **2011**, *13*, 217–225. [CrossRef]
36. Siefert, A. Incorporating intraspecific variation in tests of trait-based community assembly. *Oecologia* **2012**, *170*, 767–775. [CrossRef]
37. Benavides, R.; Scherer-Lorenzen, M.; Valladares, F. The functional trait space of tree species is influenced by the species richness of the canopy and the type of forest. *Oikos* **2019**, *128*, 1435–1445. [CrossRef]
38. Brown, J.H.; Stevens, G.C.; Kaufman, D.M. The geographic range: Size, shape, boundaries, and internal structure. *Annu. Rev. Ecol. Evol. Syst.* **1996**, *27*, 597–623. [CrossRef]
39. Pither, J. Climate tolerance and interspecific variation in geographic range size. *Proc. Biol. Sci.* **2003**, *270*, 475–481. [CrossRef]
40. Ren, L.; Guo, X.; Liu, S.; Yu, T.; Guo, W.; Eller, F. Intraspecific variation in Phragmites australis: Clinal adaptation of functional traits and phenotypic plasticity vary with latitude of origin. *J. Ecol.* **2020**, *108*, 2531–2543. [CrossRef]
41. Wang, M.; Zhang, J.; Guo, Z.; Guan, Y.; Qu, G.; Liu, J.; Guo, Y.; Yan, X. Morphological variation in *Cynodon dactylon* (L.) Pers., and its relationship with the environment along a longitudinal gradient. *Hereditas* **2020**, *157*, 4. [CrossRef]
42. Ducousso, A.; Bordacs, S. *EUFORGEN Technical Guidelines for Genetic Conservation and Use for Pedunculate and Sessile Oaks (Quercus robur and Q. petraea)*; International Plant Genetic Resources Institute: Rome, Italy, 2004; pp. 1–6.
43. Mucina, L.; Bültmann, H.; Dierßen, K.; Theurillat, J.P.; Raus, T.; Tichý, L.; Čarni, A.; Šumberová, K.; Willner, W.; Dengler, J.; et al. Vegetation of Europe: Hierarchical floristic classification system of vascular plants, bryophytes, lichens and algal communities. *Appl. Veg. Sci.* **2016**, *19*, 3–264. [CrossRef]
44. Eaton, E.G.S.D.J.; Caudullo, G.; Oliveira, S.; De Rigo, D. *Quercus robur* and *Quercus petraea* in Europe: Distribution, habitat, usage and threats. In *European Atlas of Forest Tree Species*; European Commission: Brussels, Belgium, 2016; pp. 160–163.
45. Kleinschmit, J. Intraspecific variation of growth and adaptive traits in European oak species. *Ann. For. Sci.* **1993**, *50*, 166s–185s. [CrossRef]
46. Bruschi, P.; Vendramin, G.G.; Bussotti, F.; Grossoni, P. Morphological and Molecular Diversity Among Italian Populations of *Quercus petraea* (Fagaceae). *Ann. Bot.* **2003**, *91*, 707–716. [CrossRef] [PubMed]
47. Schwarz, O. Die in der Türkei vorkommenden Bäume und Sträucher: Quercus L. (Beiträge zur Flora Klein-Asien). *Repert. Specierum Nov. Regni Veg.* **1934**, *33*, 321–338.
48. Kissling, P. Clef de détermination des chênes médioeuropéens (Quercus L.). *Berichte Schweiz. Bot. Ges.* **1980**, *90*, 2. [CrossRef]
49. Matula, R. Comparison of general tree characteristics of less known oak species *Quercus dalechampii* Ten. and *Quercus polycarpa* Schur. *J. For. Sci.* **2008**, *54*, 333–339. [CrossRef]

50. Di Pietro, R.; Viscosi, V.; Peruzzi, L.; Fortini, P. A review of the application of the name Quercus dalechampii. *Taxon* **2012**, *61*, 1311–1316. [CrossRef]
51. Fortini, P.; Di Marzio, P.; Di Pietro, R. Differentiation and hybridization of Quercus frainetto, Q. petraea, and Q. pubescens (Fagaceae): Insights from macro-morphological leaf traits and molecular data. *Plant Syst. Evol.* **2015**, *301*, 375–385. [CrossRef]
52. Opgenoorth, L.; Dauphin, B.; Benavides, R.; Heer, K.; Alizoti, P.; Mariotte, N. The GenTree platform: Growth traits and tree-level environmental data in 12 European forest tree species. *GigaScience* **2021**, *10*, 1–13. [CrossRef]
53. Benavides, R.; Carvalho, B.; Bastias, C.C.; López-Quiroga, D.; Mas, A.; Cavers, S.; Gray, A.; Albet, A.; Alía, R.; Ambrosio, O.; et al. The GenTree Leaf Collection: Inter- and intraspecific leaf variation in seven forest tree species in Europe. *Glob. Ecol. Biogeogr.* **2021**, *30*, 590–597. [CrossRef]
54. Perez-Harguindeguy, N.; Díaz, S.; Garnier, L.; Lavorel, S.; Poorter, H.; Jaureguiberry, P.; Bret-Harte, M.S.; Cornwell, W.K.; Craine, J.; Gurvich, D.E.; et al. New handbook for standardized measurement of plant functional traits worldwide. *Aust. J. Bot.* **2013**, *61*, 167–234. [CrossRef]
55. Viscosi, V. Geometric morphometrics and leaf phenotypic plasticity: Assessing fluctuating asymmetry and allometry in European white oaks (Quercus). *Bot. J. Linn. Soc.* **2015**, *179*, 335–348. [CrossRef]
56. Liu, Y.; Li, Y.J.; Song, J.L.; Zhang, R.; Yan, Y.; Wang, Y. Geometric morphometric methods of leaf shapes in two sympatric Chinese oaks: Quercus dentata Thunberg and Quercus aliena Blume (Fagaceae). *Ann. For. Sci.* **2018**, *75*, 90. [CrossRef]
57. Savriama, Y.; Klingenberg, C.P. Beyond bilateral symmetry: Geometric morphometric methods for any type of symmetry. *BMC Evol. Biol.* **2011**, *11*, 280. [CrossRef] [PubMed]
58. Rohlf, F.J. The Tps series of software. *Hystrix* **2015**, *26*, 9. [CrossRef]
59. Rohlf, F.J. *tpsUtil32*, version 1.78 [Computer Software]; Department of Ecology and Evolution, State University of New York at Stony Brook: Stony Brook, NY, USA, 2019.
60. Wickham, H. *Ggplot2: Elegant Graphics for Data Analysis*; Springer: New York, NY, USA, 2016; ISBN 978-3-319-24277-4.
61. Paradis, E.; Schliep, K. ape 5.0: An environment for modern phylogenetics and evolutionary analyses in R. *Bioinformatics* **2019**, *35*, 526–528. [CrossRef] [PubMed]
62. Wickham, H.; Averick, M.; Bryan, J.; Chang, W.; McGowan, L.D.; François, R.; Grolemund, G.; Hayes, A.; Henry, L.; Hester, J.; et al. Welcome to the tidyverse. *J. Open Source Softw.* **2019**, *4*, 1686. [CrossRef]
63. Klingenberg, C.P. Size, shape, and form: Concepts of allometry in geometric morphometrics. *Dev. Genes Evol.* **2016**, *226*, 113–137. [CrossRef]
64. Mardia, K.V.; Kent, J.T.; Bibby, J.M. *Multivariate Analysis*; Academic Press: Cambridge, MA, USA, 1979.
65. Klingenberg, C.P.; Monteiro, L.R. Distances and directions in multidimensional shape spaces: Implications for morphometric applications. *Syst. Biol.* **2005**, *54*, 678–688. [CrossRef]
66. Allen, W.J.; Meyerson, L.A.; Cummings, D.; Anderson, J.; Bhattarai, G.P.; Cronin, J.T. Biogeography of a plant invasion: Drivers of latitudinal variation in enemy release. *Glob. Ecol. Biogeogr.* **2017**, *26*, 435–446. [CrossRef]
67. Meyerson, L.A.; Cronin, J.T.; Bhattarai, G.P.; Brix, H.; Lambertini, C.; Lučanová, M.; Pyšek, P. Do ploidy level and nuclear genome size and latitude of origin modify the expression of Phragmites australis traits and interactions with herbivores? *Biol. Invasions* **2016**, *18*, 2531–2549. [CrossRef]
68. Moles, A.T.; Ackerly, D.D.; Tweddle, J.C.; Dickie, J.B.; Smith, R.; Leishman, M.R.; Westoby, M. Global patterns in seed size. *Glob. Ecol. Biogeogr.* **2007**, *16*, 109–116. [CrossRef]
69. Molina-Montenegro, M.A.; Naya, D.E. Latitudinal patterns in phenotypic plasticity and fitness-related traits: Assessing the climatic variability hypothesis (CVH) with an invasive plant species. *PLoS ONE* **2012**, *7*, e47620. [CrossRef] [PubMed]
70. Santamaría, L.; Figuerola, J.; Pilon, J.J.; Mjelde, M.; Green, A.J.; De Boer, T.; Gornall, R.J. Plant performance across latitude: The role of plasticity and local adaptation in an aquatic plant. *Ecology* **2003**, *84*, 2454–2461. [CrossRef]
71. Wang, I.J.; Glor, R.E.; Losos, J.B. Quantifying the roles of ecology and geography in spatial genetic divergence. *Ecol. Lett.* **2013**, *16*, 175–182. [CrossRef]
72. Woods, E.C.; Hastings, A.P.; Turley, N.E.; Heard, S.B.; Agrawal, A.A. Adaptive geographical clines in the growth and defense of a native plant. *Ecol. Monogr.* **2012**, *82*, 149–168. [CrossRef]
73. Zanetto, A.; Kremer, A. Geographical structure of gene diversity in *Quercus petraea* (Matt.) Liebl. I. Monolocus patterns of variation. *Heredity* **1995**, *75*, 506–517. [CrossRef]
74. Streiff, R.; Labbé, T.; Bacilieri, R.; Steinkellner, H.; Glossl, J.; Kremer, A. Within-population genetic structure in *Quercus robur* L. and *Quercus petraea* (Matt.) Liebl. assessed with isozymes and microsatellites. *Mol. Ecol.* **1998**, *7*, 317–328. [CrossRef]
75. Brullo, S.; Guarino, R.; Siracusa, G. Revisione tassonomica delle querce caducifoglie della Sicilia. *Webbia* **1999**, *54*, 1–72. [CrossRef]
76. Škvorc, Ž.; Franjić, J.; Idžojtić, M. Population structure of *Quercus pubescens* Willd. (Fagaceae) in Croatia according to morphology of leaves. *Acta Bot. Hung.* **2005**, *47*, 193–206. [CrossRef]
77. Trinajstić, I. About the problem of differentiation between the oaks *Quercus pubescens* Willd. and *Quercus virgiliana* (Ten.) Ten. *Šumarski List.* **2007**, *131*, 57–60.

78. Di Pietro, R.; Di Marzio, P.; Medagli, P.; Misano, G.; Silletti, G.N.; Wagensommer, R.P.; Fortini, P. Evidence from multivariate morphometric study of the *Quercus pubescens* complex in southeast Italy. *Bot. Serb.* **2016**, *40*, 83–90.
79. Pasta, S.; De Rigo, D.; Caudullo, G. *Quercus pubescens* in Europe: Distribution, habitat, usage and threats. In *European Atlas of Forest Tree Species*; San-Miguel-Ayanz, J., De Rigo, D., Caudullo, G., Houston Durrant, T., Mauri, A., Eds.; Publications Office of the European Union: Luxembourg, 2016; p. e01493b+.
80. Di Pietro, R.; Di Marzio, P.; Antonecchia, G.; Conte, A.L.; Fortini, P. Preliminary characterization of the *Quercus pubescens* complex in southern Italy using molecular markers. *Acta Bot. Croat.* **2020**, *79*, 15–25. [CrossRef]
81. Di Pietro, R.; Conte, A.L.; Di Marzio, P.; Fortini, P.; Farris, E.; Gianguzzi, L.; Müller, M.; Rosati, L.; Spampinato, G.; Gailing, O. Does the genetic diversity among pubescent white oaks in southern Italy, Sicily, and Sardinia islands support the current taxonomic classification? *Europ. J. For. Res.* **2021**, *140*, 355–371. [CrossRef]
82. Rydin, H.; Snoeijs, P.; Diekmann, M. (Eds.) *Swedish Plant Geography—Dedicated to Eddy van der Maarel on His 65th Birthday*; Svenska Vaxtgeografiska Sallskapet: Uppsala, Sweden, 1999; Acta Phytogeographica Suecica Volume 84; 233p.
83. Bacilieri, R.; Ducousso, A.; Kremer, A. Genetic, morphological, ecological and phenological differentiation between *Quercus petraea* (Matt.) Liebl. and *Quercus robur* L. in a mixed stand of northwest France. *Silvae Genet.* **1995**, *44*, 1–10.
84. Petit, R.J.; Bodénès, C.; Ducousso, A.G.; Kremer, A. Hybridization as a mechanism of invasion in oaks. *New Phytol.* **2003**, *161*, 151–164. [CrossRef]
85. Jensen, J.; Larsen, A.; Nielsen, L.R.; Cottrell, J. Hybridization between Quercus robur and Q. petraea in a mixed oak stand in Denmark. *Ann. For. Sci.* **2009**, *66*, 706. [CrossRef]
86. Salvini, D.; Bruschi, P.; Fineschi, S.; Grossoni, P.; Kjaer, E.D.; Vendramin, G.G. Natural hybridization between *Quercus petraea* (Matt.) Liebl. and *Quercus pubescens* Willd. within an Italian stand as revealed by microsatellite fingerprinting. *Plant Biol.* **2009**, *11*, 758–765. [CrossRef]
87. Kremer, A.; Dupouey, J.L.; Deans, J.D.; Cottrell, J.; Csaikl, U.M.; Finkeldey, R.; Espinel, S.; Jensen, J.S.; Kleinschmit, J.; Van Dam, B.; et al. Morphological variation in mixed oak stands (*Quercus robur* and *Quercus petraea*) is stable across western European populations. *Ann. For. Sci.* **2002**, *59*, 777–787. [CrossRef]
88. Curtu, A.; Gailing, O.; Finkeldey, R. Evidence for hybridization and introgression within a species-rich oak (*Quercus* spp.) community. *BMC Evol. Biol.* **2007**, *7*, 218. [CrossRef]
89. Neophytou, C.; Aravanopoulos, F.A.; Fink, S.; Dounavi, A. Detecting interspecific and geographic differentiation patterns in two interfertile oak species (*Quercus petraea* (Matt.) Liebl. and *Q. robur* L.) using small sets of microsatellite markers. *For. Ecol. Manag.* **2010**, *259*, 2026–2035. [CrossRef]
90. Craine, J.M.; Elmore, A.J.; Aidar, M.P.; Bustamante, M.; Dawson, T.E.; Hobbie, E.A.; Kahmen, A.; Mack, M.C.; McLauchlan, K.K.; Michelsen, A.; et al. Global patterns of foliar nitrogen isotopes and their relationships with climate, mycorrhizal fungi, foliar nutrient concentrations, and nitrogen availability. *New Phytol.* **2009**, *183*, 980–992. [CrossRef]
91. Wangari, E.G.; Mwanake, R.M.; Houska, T.; Kraus, D.; Kikowatz, H.M.; Wolf, B.; Gettel, G.M.; Breuer, L.; Ambus, P.; Kiese, R.; et al. Spatial-temporal patterns of foliar and bulk soil 15N isotopic signatures across a heterogeneous landscape: Linkages to soil N status, nitrate leaching, and N2O fluxes. *Soil Biol. Biochem.* **2024**, *199*, 109609. [CrossRef]
92. Evans, R.D. Physiological mechanisms influencing plant nitrogen isotope composition. *Trends Plant Sci.* **2001**, *6*, 121–126. [CrossRef] [PubMed]
93. Nakamura, T.; Yabe, K.; Matsubara, T.; Osaki, M. Variations in the nitrogen isotope abundance of foliage in a tropical evergreen species (*Combretocarpus rotundatus*) relative to leaf position and habitat. *Tropics* **2012**, *21*, 119–126. [CrossRef]
94. Rivas-Martínez, S.; Penas, A.; Díaz, T. *Bioclimatic Map of Europe*; Cartographic Service, University of León: León, Spain, 2001.
95. Di Pietro, R.; Conte, A.L.; Di Marzio, P.; Gianguzzi, L.; Spampinato, G.; Caldarella, O.; Fortini, P. A multivariate morphometric analysis of diagnostic traits in southern Italy and Sicily pubescent oaks. *Folia Geobot.* **2020**, *55*, 163–183. [CrossRef]
96. Bartolucci, F.; Peruzzi, L.; Galasso, G.; Albano, A.; Alessandrini, A.; Ardenghi, N.M.G.; Astuti, G.; Bacchetta, G.; Ballelli, S.; Banfi, E.; et al. An updated checklist of the vascular flora native to Italy. *Plant Biosyst.* **2018**, *152*, 179–303. [CrossRef]
97. Di Pietro, R.; Fortini, P.; Ciaschetti, G.; Rosati, L.; Viciani, D.; Terzi, M. A revision of the syntaxonomy of the Apennine-Balkan *Quercus cerris* and *Q. frainetto* forests and correct application of the name Melittio-Quercion frainetto. *Plant Biosyst.* **2020**, *154*, 887–909. [CrossRef]
98. Quercus, A.-F.J. *Flora Ibérica II*; Castroviejo, S., Laínz, M., López González, G., Montserrat, P., Muñoz Garmendia, F., Paiva, J., Villar, L., Eds.; CSIC: Madrid, Spain, 1990.
99. Peppe, D.J.; Royer, D.L.; Cariglino, B.; Oliver, S.Y.; Newman, S.; Wright, I.J. Sensitivity of leaf size and shape to climate: Global patterns and paleoclimatic applications. *New Phytol.* **2011**, *190*, 724–739. [CrossRef]
100. Liu, J.; Zhao, Y.; Zhang, C.; Xu, J.; Wu, Y. Global Patterns of Leaf Size and Its Relationship with Climate. *Nat. Commun.* **2021**, *12*, 1234.
101. Parkhurst, D.F.; Loucks, O.L. Optimal leaf size in relation to environment. *J. Ecol.* **1972**, *60*, 505–537. [CrossRef]

102. Niinemets, Ü.; Kull, K. Leaf weight per area and leaf size of 85 Estonian woody species in relation to shade tolerance and light availability. *For. Ecol. Manag.* **1994**, *70*, 1–10. [CrossRef]
103. Bussotti, F.; Bettini, D.; Grossoni, P.; Mansuino, S.; Nibbi, R.; Soda, C.; Tani, C. Structural and functional traits of *Quercus ilex* in response to water availability. *EEB Environ. Exp. Bot.* **2002**, *47*, 11–23. [CrossRef]
104. Fortini, P.; Di Marzio, P.; Conte, A.L.; Antonecchia, G.; Proietti, E.; Di Pietro, R. Morphological and molecular results from a geographical transect focusing on *Quercus pubescens*/*Q. virgiliana* ecological-altitudinal vicariance in peninsular Italy. *Plant Biosyst.* **2022**, *156*, 1498–1511. [CrossRef]
105. Mátyás, V. Taxa nova Quercuum Hungariae. *Acta Bot. Acad. Sci. Hung.* **1970**, *16*, 329–361.
106. Magic, D. *Quercus* L. In *Benčat' F. et al Flóra Slovenska*; Goliašová, K., Michalková, E., Eds.; V/3; Veda: Bratislava, Slovakia, 2006; pp. 108–143.
107. Filipova, E.; Asenov, A. Review on *Quercus dalechampii* Ten. and *Quercus petraea* (Mattuschka) Liebl. in the Vegetation of Bulgaria. In *Annual of Sofia University "St. Kliment Ohridski" Faculty of Biology Book 2 Botany*; St. Kliment Ohridski University Press: Sofia, Bulgaria, 2016; Volume 100, pp. 116–123. [CrossRef]
108. Kučera, P. *Quercus banatus* grows in Slovenia. *Thaiszia—J. Bot.* **2018**, *29*, 61–69. [CrossRef]
109. Kaplan, Z.; Danihelka, J.; Chrtek, J.; Prančl, J.; Grulich, V.; Jelínek, B.; Úradníček, L.; Řepka, R.; Šmarda, P.; Vašut, R.J.; et al. Distributions of vascular plants in the Czech Republic Part 11. *Preslia* **2022**, *94*, 335–427. [CrossRef]
110. Bennett, K.D.; Tzedakis, P.C.; Willis, K.J. Quaternary refugia of north European trees. *J. Biogeogr.* **1991**, *18*, 103–115. [CrossRef]
111. Hewitt, G.M. Post-glacial re-colonization of European biota. *Biol. J. Linn. Soc.* **1999**, *68*, 87–112. [CrossRef]
112. Médail, F.; Diadema, K. Glacial refugia influence plant diversity patterns in the Mediterranean Basin. *J. Biogeogr.* **2009**, *36*, 1333–1345. [CrossRef]
113. Di Pietro, R.; Quaranta, L.; Mattioni, C.; Simeone, M.C.; Di Marzio, P.; Proietti, E.; Fortini, P. Chloroplast haplotype diversity in the white oak populations of the Italian Peninsula, Sicily, and Sardinia. *Forests* **2024**, *15*, 864. [CrossRef]
114. Olalde, M.; Herrán, A.; Espinel, S.; Goicoechea, P.G. White oaks phylogeography in the Iberian Peninsula. *For. Ecol. Manag.* **2002**, *156*, 89–102. [CrossRef]
115. Fineschi, S.; Taurchini, D.; Grossoni, P.; Petit, R.J.; Vendramin, G.G. Chloroplast DNA variation of white oaks in Italy. *For. Ecol. Manag.* **2002**, *156*, 103–114. [CrossRef]
116. Vila-Viçosa, C.; Gonçalves, J.; Honrado, J.; Lomba, Â.; Almeida, R.S.; Vázquez, F.M.; Garcia, C. Late Quaternary range shifts of marcescent oaks unveil the dynamics of a major biogeographic transition in southern Europe. *Sci. Rep.* **2020**, *10*, 21598. [CrossRef] [PubMed]
117. Fady, B.; Esposito, E.; Abulaila, K.; Aleksic, J.M.; Alia, R.; Alizoti, P.; Apostol, E.-N.; Aravanopoulos, P.; Ballian, D.; Kharrat, M.B.D.; et al. Forest genetics research in the Mediterranean Basin: Bibliometric analysis, knowledge gaps, and perspectives. *Curr. For. Rep.* **2022**, *8*, 277–298. [CrossRef]
118. Šijačić-Nikolić, M.; Kerkez Janković, I.; Jovanović, M.; Milovanović, J.; Aleksić, J.M. Genetic diversity and genetic structure of three sympatric oak species in the Serbian landscape of outstanding features "Kosmaj" assessed by nuclear microsatellites. *SEEFOR* **2023**, *14*, 117–127. [CrossRef]
119. Fortini, P.; Di Pietro, R.; Proietti, E.; Cardoni, S.; Quaranta, L.; Simeone, M.C. Dissecting the continuum and unraveling the phylogeographic knot of plastid DNA in European white oaks (Quercus sect. Quercus): Ancient signatures and multiple diversity reservoirs. *Eur. J. For. Res.* **2023**, *143*, 107–127. [CrossRef]
120. Menitsky, Y.L. *Oaks of Asia*; Science Publishers of Enfield Press: Enfield, NH, USA, 2005.
121. Ekhvaia, J.; Simeone, M.C.; Silakadze, N.; Abdaladze, O. Morphological diversity and phylogeography of the Georgian durmast oak (*Quercus petraea* subsp. iberica) and related Caucasian oak species in Georgia (South Caucasus). *Tree Genet. Genomes* **2018**, *14*, 17. [CrossRef]
122. Borazan, A.; Babac, M.T. Morphometric leaf variation in oaks (Quercus) of Bulu, Turkey. *Ann. Bot. Fenn.* **2003**, *40*, 233–242.
123. Panahi, P.; Jamzad, Z.; Pourmajidian, M.R.; Fallah, A.; Pourhashemi, M. Foliar epidermis morphology in Quercus (subgenus Quercus, section Quercus) in Iran. *Acta Bot. Croat.* **2012**, *71*, 95–113. [CrossRef]